Dalton Transactions

An international journal of inorganic chemistry

Accepted Manuscript

This article can be cited before page numbers have been issued, to do this please use: R. Li, Y. Ma, X. Hu, W. Wu, X. Wu, C. Dong, S. Shi and Y. Lin, *Dalton Trans.*, 2020, DOI: 10.1039/D0DT01877E.




ROYAL SOCIETY OF CHEMISTRY

rsc.li/dalton

Journal Name ARTICLE

ARTICLE

View Article Online
DOI: 10.1039/D0DT01877E

# [Ru(phen)$_2$podppz]$^{2+}$ significantly inhibits glioblastoma growth in vitro and vivo with fewer side-effects compared with cisplatin

Received 00th January 20xx,
Accepted 00th January 20xx

DOI: 10.1039/x0xx00000x

Ruihao Li[#a], Yabin Ma[#b], Xiaochun Hu[a], Wenjing Wu[a], Xuewen Wu[a], Chunyan Dong[a], Shuo Shi[*a], Yun Lin[*a]

To overcome the acquired resistance and the significant side-effects of the reported drugs, four new ruthenium (II) complexes with alkynyl (Ru1, Ru2, Ru3, Ru4) were designed and synthesized. Ru1, Ru2, Ru3 and Ru4 were characterized by ESI-MS, $^1$H NMR, $^1$H-$^1$H COSY NMR and elemental analysis. Compared with Ru2, Ru3, Ru4 and cisplatin, the anti-tumor experiments in vitro and vivo confirmed that Ru1 could most effectively inhibit tumor growth. In the experiments of safety evaluation in vivo, Ru1 could avoid any detectable side-effects compared with cisplatin. DNA binding experiments and cell cycle experiments showed that Ru1 exhibited the strongest DNA binding ability and interfered with the cell cycle by inserting DNA to inhibit tumor growth. The study demonstrated Ru1 owned potential to be an exciting new drug candidate for glioblastoma treatment.

## Introduction

Glioblastoma multiforme (GBM), emanated from the glial cell, is the most prevailing malignant tumor of the central nervous system and the most aggressive form of glioma.[1] The median survival is less than 2 years with the current standard treatment of maximal safe resection, combination of chemotherapy given with radiation therapy.[2] Temozolomide (TMZ) was used to treat GBM for over a decade, but its therapeutic effects are limited by acquired resistance.[3]

In 1969, Bamett Rosenberg, American biophysicist, accidentally discovered the anti-tumor ability of cisplatin (DDP), and DDP gradually became the first-line drug in clinical practice.[4, 5] The major issues of DDP chemotherapy are the resistance and side effects,[6-9] such as renal toxicity, myelosuppression, nausea, vomiting, and toxicity, which limits its use in tumor therapy. Ruthenium and platinum belong to 8 subgroup of transition metal elements and own similar nature,[10] but the richer valences (II, III, IV) of ruthenium result in more diverse physical and chemical properties.[11-13] Recently, the good biocompatibility and powerful anti-tumor effect of ruthenium (II) complexes provide a new idea and a good alternative to platinum drugs. [14-21]

Ru (II) complexes can intercalate into the structure of double-stranded DNA to interfere with the self-replication of DNA, [22, 23] thus affecting the progress of cell cycle and inhibiting division and proliferation of tumor cells, and finally inducing the apoptosis of tumor cells. It can also interfere cellular transcription processes by inserting DNA, which eventually lead to preventing RNA polymerases from binding with DNA and inhibiting the growth of tumor cells.[24,25]

Although numerous previous studies have shown the anti-tumor effects and the ability of fluorescence imaging of Ru (II) complexes in vitro and vivo experiments,[26, 27] Ru (II) complexes have not been approved for clinical use. Recent study indicated that alkynyl groups could not only improve the ability of substances to enter cells but increase the ability of Ru (II) complexes to bind to DNA. [28-31]

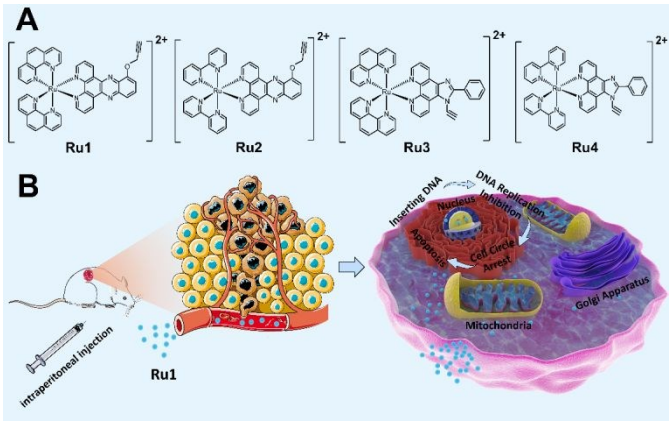


Scheme. 1 (A) structures of Ru (II) complexes. (B) The schematic description of the anti-tumor mechanism of Ru1.

[a.] *Shanghai East Hospital, Shanghai Key Lab of Chemical Assessment and Sustainability, School of Chemical Science and Engineering, Tongji University, 1239 Siping Road, 200092 Shanghai, P.R. China.*
[b.] *Department of Pharmacy, Shanghai East Hospital, Tongji University, Shanghai 200120, PR China*
[#] Contribute equally to this work
E-mail: ylin@tongji.edu.cn, shishuo@tongji.edu.cn
Electronic Supplementary Information (ESI) available: [details of any supplementary information available should be included here]. See DOI: 10.1039/x0xx00000x

In this study, we have synthesized and characterized four new ruthenium (II) complexes with alkynyl, $[Ru(phen)_2po\text{-}dppz]^{2+}$, $Ru(bpy)_2podppz]^{2+}$, $[Ru(phen)_2ppip]^{2+}$, $[Ru(bpy)_2ppip]^{2+}$. In vitro studies verified the long-term stability in phosphate-buffered saline (PBS) and water. The anti-tumor mechanism of Ru1 was investigated via DNA binding experiments and cell cycle assay. In vivo safety evaluation demonstrated that Ru1 could avoid any detectable side-effects compared with cisplatin. In vivo anti-tumor GBM models, Ru1 could effectively inhibit tumor growth, suggested that Ru1 could be utilized as a potential drug for GBM treatment.

## Results and discussion

### Synthesis and Characterization

Initially, the compounds pip, hdppz, cis-$[Ru(phen)_2Cl_2]\cdot 2H_2O$ and cis-$[Ru(bpy)_2Cl_2]\cdot 2H_2O$ were synthesized according to the literature references.[32-35] Subsequently, the reported complexes RA, RB, RC and RD were similarly obtained according to the literatures (Fig.S1).[34-38]

The synthetic route to the alkynyl complexes is summarized in Scheme 2. RA, RB, RC and RD were individually reacted with propargyl bromide in the presence of anhydrous potassium carbonate in DMF resulting in the formation of alkynyl ($[Ru(phen)_2podppz]^{2+}$, $Ru(bpy)_2podppz]^{2+}$, $[Ru(phen)_2ppip]^{2+}$, $[Ru(bpy)_2ppip]^{2+}$ (Ru1, Ru2, Ru3, Ru4) respectively, in very good yield. All the new compounds were fully characterized by $^1H$ NMR, $^1H$-$^1H$ COSY, TOF-MS, and elemental analysis (Fig.S2-S5).

These complexes exhibit a weak solubility in water, but show a high solubility in DMSO. All Ru (II) complexes displayed remarkable stability in PBS or water (containing 0.5% DMSO) at 298 K for at least 5 days, as verified by UV–Vis spectroscopy (Fig. S6).

### UV–Vis Absorption Titration

To clarify the nature of the different cytotoxicities induced by complexes, UV absorption spectroscopy studies were carried out to investigate the DNA binding ability of Ru (II) complexes. When calf-thymus DNA (CT-DNA) was added into Ru1 solution, obvious hypochromism (H) was observed for both intra-ligand charge transfer (ILCT) (λ = 250-260 nm) band and metal-to-ligand charge transfer (MLCT) (λ = 400-420 nm). However, slight hypochromism was observed for the other complexes. The extent of the hypochromism commonly parallels the intercalative binding affinity. These results demonstrated that Ru1 exhibits the strongest DNA binding ability (Fig.S8).

Since the octahedral complex binds to DNA in three dimensions, both its ancillary ligand and intercalative ligand can tune the DNA binding affinity.[39-41] Increasing the surface area of the ancillary ligand and intercalative ligand leads to a substantially increased intercalative binding affinity. On-going from the ancillary ligand phen to bpy, the hydrophobicity of the ancillary ligand phen of Ru1 is greater than that of the bpy ligand of Ru2. Meanwhile, the surface area for intercalative ligand podppz is bigger than ppip, which is advantageous to DNA binding of Ru1, too. Therefore, synthetically considering these factors, Ru1 exhibiting the strongest DNA binding ability and the best anti-proliferative effect could be well understood. Meanwhile, the results showed a significant difference in the ability of DDP and Ru1 to reduce cell viability. The antitumor ability of Ru1 is the most prominent candidate among the four new synthesized Ru (II) complexes. Therefore, further experiments were performed to assess the antitumor capacity of Ru1.

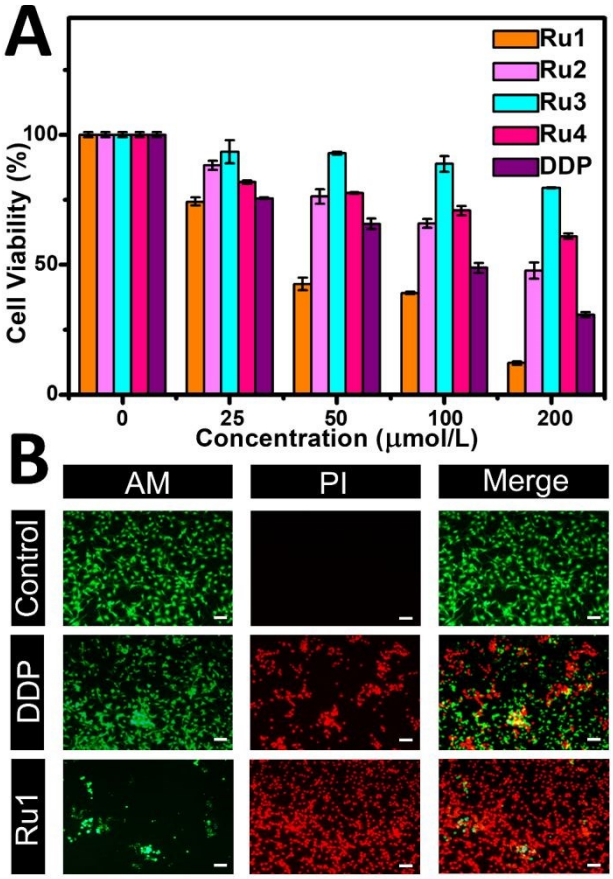


Fig.1 (A) In vitro cytotoxicity of Ru1, Ru2, Ru3, Ru4 and DDP against U87 MG cells with different drug dosages for 24 h via the CCK-8 assay. (B) Fluorescent inverted microscope images of U87 MG cells treated with PBS, DDP and Ru1 for 24 h. Live and dead cells were stained by Calcein AM (AM)/Propidium Iodide (PI) for 30 min and presented in green and red colors in those images, respectively. Scale bar is 100 μm.

### In Vitro Toxicity

To screen the most powerful anti-tumor capability of Ru (II) complexes, we assess the cytotoxicity of them against GBM in vitro and vivo. The in vitro cytotoxicity of Ru1, Ru2, Ru3, Ru4 and DDP against U87 MG cells was investigated by the CCK-8 assay. Compared with Ru2, Ru3, Ru4 and DDP, Ru1 exhibited the strongest anti-proliferative effect due to the strongest DNA binding ability inducing cell apoptosis and inhibiting cell cycle (Fig.1A). Because of the poor solubility of Ru complexes in water, these complexes were first dissolved in DMSO and then diluted into the test solution appropriately. Meanwhile, the vitro cytotoxicities of 0.25% and 0.5% DMSO in controlled buffers against U87 MG cells were also invested. The results confirmed

View Article Online
DOI: 10.1039/D0DT01877E



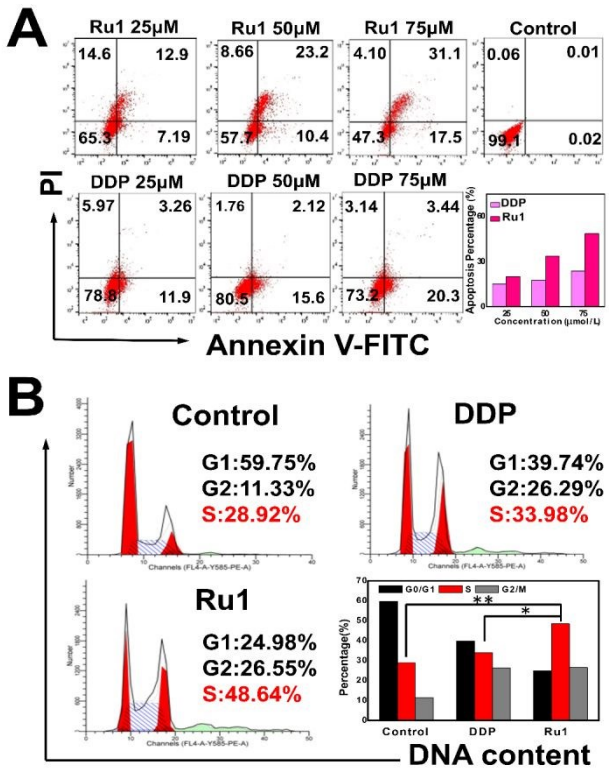


Fig.2 Cellular apoptosis and cell cycle analysis in U87 MG cells in response to PBS, DDP and Ru1. (A) Flow cytometry of 5 μL Annexin V and 5 μL PI labelled U87 MG cells exposed to PBS, DDP or Ru1 for 24 h. (B) Flow cytometry of PI labelled U87 MG cells incubated with PBS, DDP, or Ru1 for 24 h. Quantitative flow cytometry analysis of cell cycle ratios. (Single asterisks indicate $p < 0.05$, double asterisks indicate $p < 0.01$, and triple asterisks indicate $p < 0.001$).

that the addition of small amount of DMSO was not toxic to U87, and the anti-tumor effect was caused by the ruthenium complexes themselves (Fig.S7).

**Live & Dead Viability Assay**

Moreover, to observe the anti-proliferative ability of DDP and Ru1, U87 MG cells were stained with AM/PI after administered with the same concentration of DDP and Ru1. It was found that most U87 MG cells remain alive (represented by green color) after treatment with DDP, suggesting DDP has no significant efficacy on damaging of U87 (Fig.1B). In contrast, the treatment with Ru1 resulted in a large quantity of dead cells (represented by red color). This result sufficiently demonstrates Ru1 has stronger ability of killing U87 MG cells than DDP.

**Cellular Apoptosis**

Flow cytometry was used to continue our exploration on the mechanism of cytotoxicity of Ru1 against tumor cells. Apoptotic and necrotic cells were detected in U87 MG cells via dual fluorescence staining of Annexin V /PI. As shown in Fig.2A, only 23.7% of U87 MG cells were apoptotic after administered with DDP (75 μmol/L). While almost 48.6% of U87 MG cells were apoptotic after treated with an equal concentration of Ru1. This result demonstrated that Ru1 owned the stronger ability of inducing cellular apoptosis of U87 than DDP, which was consistent with the results of cytotoxicity tests.

**Cell Cycle Analysis**

Completion of cell cycle is crucial for DNA replication. And the dynamic balance of cell cycle activities is an important factor to maintain the stable transmission of genetic information. To further investigate the mechanisms of inhibiting tumor cell proliferation of Ru1, the effect of Ru1 and DDP on the cell cycle were assessed in U87 MG cells by flow cytometry. 33.9% of cells were blocked in the S phase by DDP, while 48.6% of cells treated with Ru1 in the S phase were observed, which confirmed that Ru1 and DDP could play an anti-tumor role through inhibition of cell cycle stranded in the S phase (Fig.2B). Moreover, Ru1 showed more excellent inhibition ability of the cell cycle than DDP. Taken together, these results demonstrated that DNA damage caused by Ru1 can efficiently inhibit cell cycle arrest and induce cellular apoptosis.

**In Vivo Anti-Tumor Study**

To investigate the in vivo anti-tumor efficacy of Ru1, mice bearing subcutaneous U87 MG tumor were treated with PBS, DDP and Ru1 at a single dosage of 5 mg/kg via intraperitoneal injection. The in vivo antitumor experiment further confirmed excellent tumor growth inhibition achieved by Ru1 (Fig.3A). Tumor volumes of mice were measured every 2 days for 10 days after administration. Ru1 could inhibit tumor growth more effectively, comparing with the PBS group and the DDP group (Fig.3B).

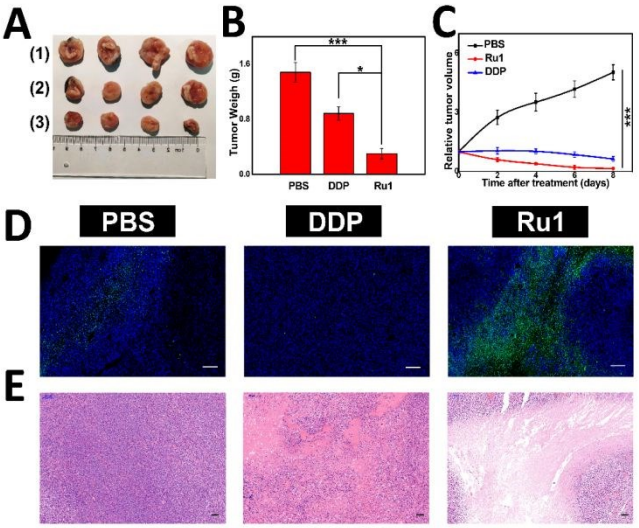


Fig.3 (A) The image of tumors isolated from the nude mice. (3 groups, (1) PBS, (2) DDP, (3) Ru1). (B) Tumor growth curves and (C) histogram of average tumor weight measured on day 10 after various treatments. (D) Apoptotic tumor cells in tumor sections were stained with TUNEL (green) observed by fluorescence microscopy. Cell nuclei were stained with DAPI (blue). (E) H&E stained of tumors of mice from each group (Single asterisks indicate $p < 0.05$, double asterisks indicate $p < 0.01$, and triple asterisks indicate $p < 0.001$). Scale bars: 100 μm.

View Article Online
DOI: 10.1039/D0DT01877E

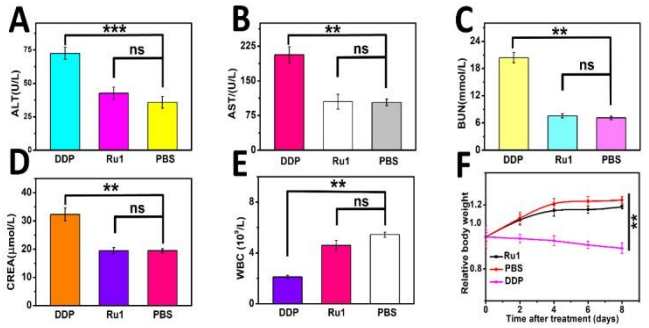


Fig.4 In vivo toxicity and safety studies of DDP and Ru1 in nude mice. Mice were injected with PBS, DDP and Ru1 at a single dosage of 5 mg per kilogram of animal body weight. (A) ALT and (B) AST levels represent liver function. (C) BUN and (D) CREA represent kidney function. (E) WBC counts. Data were expressed as mean ± SD (n=3). (F) The relative body weight of mice. Data were expressed as mean ± SD (n=4). (Single asterisks indicate $p < 0.05$, double asterisks indicate $p < 0.01$, and triple asterisks indicate $p < 0.001$).

The tumor weight was measured to assess the therapeutic effect, too. The results were consistent with the tumors volume as expected: tumor weights for the Ru1 group and DDP group on day 10 were 300 ± 17 mg and 770 ± 18 mg, respectively (Fig.3C). The sections from tumors in each group were stained with TUNEL[42] for the evaluation of apoptosis at the histological level (Fig.3D). Compared with the DDP groups, tumors treated with Ru1 showed the higher apoptosis due to the suppression of DNA replication and transcription. H&E staining of tumors in mice from each group showed the necrosis degeneration of tumor cells for the Ru1 group was more obvious than the other groups (Fig.3E).

### In Vivo Safety Evaluation of DDP and Ru1

To investigate the in vivo safety and biocompatibility of Ru1 and DDP, the blood of all mice was collected after treatment on day 10 for biochemistry tests and blood routine examination. Blood biochemistry analysis showed that blood urea nitrogen (BUN), creatinine (CREA), aspartate aminotransferase (AST) and alanine aminotransferase (ALT) levels of mice treated with DDP were significantly higher than that of the other two (Fig.4A-D). There was no significate difference in alkaline phosphatase (ALP) between DDP group and other groups (Fig.S9). According to the results, the function of liver and kidney was obviously damaged in DDP group. No significant hematological toxicity was caused by Ru1. The mice treated with DDP presented a significant decrease in white blood cell (WBC) count (Fig.4E), suggesting the occurrence of myelosuppression, which is one of the main side-effects of DDP. The decrease in WBC count was significantly attenuated with Ru1 treatment. Other major indicators of blood routine were not statistically different among these three groups (Fig.S10). We also measured the changes of body weight to evaluate the systemic toxicity of the chemotherapeutic agents. Mice treated with Ru1 presented no significate weight loss compared with the PBS group, whereas the therapy of DDP reduced the weight of mice noticeably (Fig.4F).

### Histopathological Examination

H&E staining of the major organs showed that liver damage caused by DDP, including cells edema, small vacuolar degeneration in cytoplasm, pyknosis in cell nucleus via our histological observations. There was no abnormality of the renal pathology observed in the DDP group, which only caused renal dysfunction instead of obvious tissue damage. The Ru1 group showed negligible pathological injury in line with the PBS group (Fig.5A–E). Biochemistry tests, blood routine examination and histological results further confirmed the lower systemic toxicity and better in vivo safety of Ru1.

## Experimental section

### Materials

Cisplatin was obtained from Dalian Meilun Biotechnology Co. LTD. (Dalian, China). Phosphate Buffered Saline (PBS), Dulbecco's Modified eagle's medium (DMEM/high glucose) and trypsin-EDTA were purchased from HyClone (USA). Fetal bovine serum (FBS) were obtained from Clarkbio FB25015 (Shanghai, china). Cell counting Kit-8 (CCK-8), Annexin V-FITC Apoptosis Detection Kit, Cell Cycle Detection Kit and Live & Dead Viability Assay Kit were purchased from Jiangsu KeyGEN BioTECH Corp. Ltd. (Jiangsu, China). Ethanol and dimethyl sulfoxide (DMSO) were obtained from Sinopharm Chemical Reagent Co. Ltd. BALB/c nude mice were purchased from Silaike Experimental Animal Centre (Shanghai, China). This study was approved by the Ethics Committee of Tongji University.

Physical measurements

$^1$H NMR spectra was collected at 300 K on a Bruker spectrometer. $^1$H-$^1$H COSY NMR spectra were recorded on a Bruker AV-400M spectrometer. Mass spectra were measured on an Agilent TOF-G6230B mass spectrometer. Microanalysis of elements (C, H, and N) was carried out using a Thermo Flash 2000 analyzer.

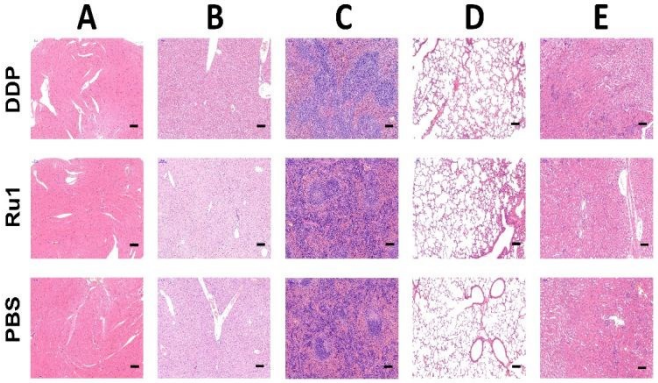


Fig.5 (A-E) H&E stained histological sections. (A) Heart, (B) liver, (C) spleen, (D) lung and (E) kidney of mice from each group were observed. Scale bars: 100 μm.

### Synthesis and characterization

**[Ru(phen)$_2$podppz]$^{2+}$ (Ru1)**

[Ru(phen)$_2$hdppz]$^{2+}$ (RA) was prepared and characterized according to the literature.[36] Firstly, RA (0.4 mmol, 420 mg) and $K_2CO_3$ (0.4 mmol, 55 mg) were suspended in DMF (4 mL). Then,

View Article Online
DOI: 10.1039/D0DT01877E

ARTICLE

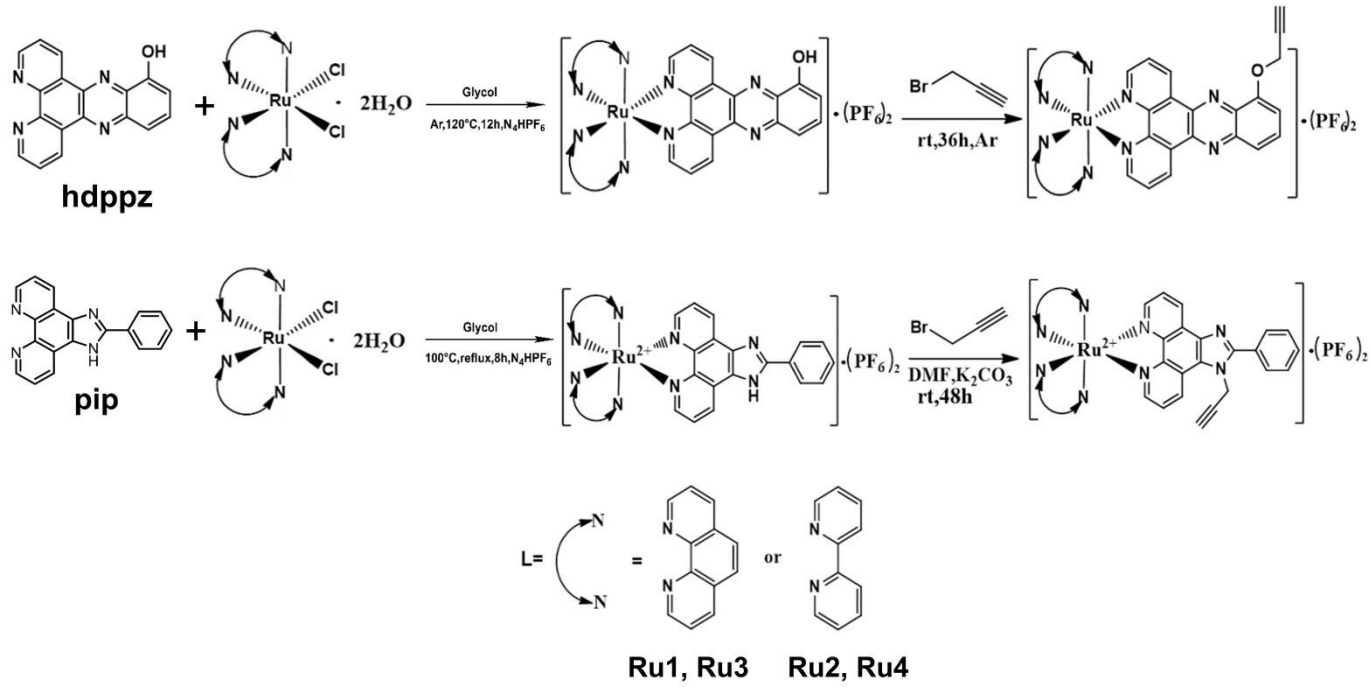


Scheme. 2 Synthetic route for Ru1, Ru2, Ru3 and Ru4

propargyl bromide (0.8 mmol, 66 μL) was added and the reaction mixture was stirred at room temperature for 36 h under argon. Upon addition of 10 mL water, the precipitated complex was washed with water (4×30 mL), and purified by chromatography over alumina by using MeCN as eluent, yield: about 55% (236 mg) .$^1$H NMR (600MHz, $CD_3CN$) δ 9.42 (dd, *J* =8.2, 1.0 Hz, 1H), 9.26 (dd, *J* = 8.2, 0.9 Hz, 1H), 8.71 (dd, *J* = 8.3, 1.2 Hz, 1H), 8.69 – 8.65 (m, 3H), 8.40 (dd, *J* = 5.3, 1.2 Hz, 1H), 8.34 – 8.30 (m, 4H), 8.27 (dd, *J* = 5.3, 1.2 Hz, 1H), 8.17 (dd, *J* = 5.4, 1.2 Hz, 1H), 8.08 (dddd, *J* = 21.9, 16.4, 6.9, 4.5 Hz,4H), 7.98 (dd, *J* = 8.7, 0.9 Hz, 1H), 7.80 (dd, *J* = 8.2, 5.3 Hz, 1H), 7.75 – 7.68 (m, 4H), 7.57 (dd, *J* = 7.8, 0.8 Hz, 1H), 7.51 (dd, *J* = 8.2, 5.4 Hz, 1H), 5.18 (d, *J* = 2.4 Hz, 2H), 3.02 (t, *J* = 2.4 Hz, 1H). TOF-MS for $C_{45}H_{28}N_8ORu^{2+}$: Calcl.798.14, found m/z 399.0804 ($M^{2+}$/2). Anal. data for $C_{45}H_{28}F_{12}N_8OP_2Ru$: calc (%): C, 49.69; H, 2.59; N, 10.30. found (%): C, 49.55; H, 2.57; N, 10.27.

**Ru(bpy)$_2$podppz]$^{2+}$ (Ru2)**

[Ru(bpy)$_2$hdppz]$^{2+}$ (RB) was prepared and characterized according to the literature.[37] Ru2 was synthesized similarly to Ru1. RB (0.4 mmol, 400 mg) and $K_2CO_3$ (0.4 mmol, 55 mg) were suspended in DMF (4 mL). Then, propargyl bromide (0.8 mmol, 66 μL) was added and the reaction mixture was stirred at room temperature for 36 h under argon. Upon addition of 10 mL water, the precipitated complex was washed with water, and purified by chromatography over alumina by using MeCN as eluent, yield: 52.5% (215 mg). $^1$H NMR (600MHz, $CD_3CN$) δ 9.42 (dd, *J* = 8.2, 1.1 Hz, 1H), 9.27 (dd, *J* = 8.2, 1.0 Hz, 1H), 8.69 – 8.57 (m, 4H), 8.24 (dd, *J* = 5.3, 1.2 Hz, 1H), 8.23 – 8.16 (m, 3H), 8.09 (dddd, *J* = 16.4, 14.3, 8.2, 4.6 Hz, 3H), 8.00 – 7.91 (m, 4H), 7.87 (dd, *J* = 8.2, 5.3 Hz, 1H), 7.78 (dd, *J* = 5.7, 0.7 Hz, 1H), 7.71 (dd, *J* = 8.2, 5.3 Hz, 1H), 7.61 – 7.49 (m, 3H), 7.42 (ddd, *J* = 7.3, 5.8, 1.2 Hz, 1H), 7.34 (ddd, *J* = 7.3, 5.8, 1.2 Hz, 1H), 5.17 (d, *J* = 2.4 Hz, 2H), 3.03 (t, *J* = 2.4 Hz, 1H). TOF-MS for $C_{41}H_{28}N_8ORu^{2+}$: Calcl.750.14 found m/z 375.07 ($M^{2+}$/2). Anal. data for $C_{41}H_{28}F_{12}N_8OP_2Ru$: calc (%): C, 47.36; H, 2.71; N, 10.78. found (%): C, 47.45; H, 2.69; N, 10.81.

**[Ru(phen)$_2$ppip]$^{2+}$ (Ru3)**

[Ru(phen)$_2$pip]$^{2+}$ (RC) was similarly obtained according to the literature.[38] Firstly, RC (0.4 mmol, 419 mg) and $K_2CO_3$ (0.4 mmol, 55 mg) were suspended in DMF (4 mL). Propargyl bromide (0.8 mmol, 66 μL) was then added and the reaction mixture was stirred at room temperature for 48 h under argon. Upon addition of 10 mL water, the precipitated complex was washed with water, and purified by chromatography over alumina by using MeCN as eluent. yield 50% (0.2I7 mg). $^1$H NMR (600MHz, DMSO) δ 9.19 (d, *J* = 8.6 Hz, 1H), 9.10 (d, *J* = 7.3 Hz, 1H), 8.82 – 8.76 (m, 4H), 8.41 (d, *J* = 5.4 Hz, 4H), 8.19 (d, *J* = 5.3 Hz, 1H), 8.10 (t, *J* = 5.0 Hz, 4H), 8.08 (d, *J* = 5.4 Hz, 1H), 7.97 – 7.94 (m, 2H), 7.90 (dd, *J* = 8.6, 5.3 Hz, 1H), 7.83 – 7.71 (m, 8H), 5.62 – 5.51 (m, 2H), 3.89 (t, *J* = 2.3 Hz, 1H). TOF-MS for $C_{46}H_{30}N_8Ru^{2+}$: Calcl.796.16, found m/z 398.08 ($M^{2+}$/2). Anal. data for $C_{46}H_{30}F_{12}N_8P_2Ru$: calcd (%): C, 50.88; H, 2.79; N, 10.32. found (%): C, 50.95, H, 2.80; N, 10.34.

**[Ru(bpy)$_2$ppip]$^{2+}$ (Ru4)**

[Ru(bpy)$_2$pip]$^{2+}$ (RD) was prepared and characterized according to the literature.[35] Ru4 was synthesized similarly to Ru3. RD (0.4 mmol, 400 mg) and $K_2CO_3$ (0.4 mmol, 55 mg) were suspended in DMF (4 mL). Propargyl bromide (0.8 mmol, 66 μL) was added

and the reaction mixture was stirred at room temperature for 48 h under argon. Upon addition of 10 mL water, the precipitated complex was washed with water, and purified by chromatography over alumina by using MeCN as eluent. yield about 55.8% (223 mg). $^1$H NMR (600MHz, DMSO) δ 9.22 (d, *J* = 8.6 Hz, 1H), 9.14 (d, *J* = 8.2 Hz, 1H), 8.90 (dd, *J* = 8.2, 3.9 Hz, 2H), 8.86 (dd, *J* = 11.0, 8.5 Hz, 2H), 8.24 (t, *J* = 7.9 Hz, 2H), 8.17 – 8.09 (m, 4H), 8.02 (dd, *J* = 8.5, 5.3 Hz, 1H), 7.97 – 7.93 (m, 3H), 7.87 (t, *J* = 4.8 Hz, 2H), 7.76 – 7.71 (m, 3H), 7.66 (d, *J* = 5.5 Hz, 1H), 7.63 – 7.58 (m, 3H), 7.36 (dt, *J* = 17.1, 6.7 Hz, 2H), 5.57 (ddd, *J* = 48.3, 19.3, 2.2 Hz, 2H), 3.90 (t, *J* = 2.3 Hz, 1H). TOF-MS for $C_{42}H_{30}N_8Ru^{2+}$: Calcl.748.16, found m/z 374.08 ($M^{2+}$/2). Anal. data for $C_{42}H_{30}F_{12}N_8P_2Ru$: calc (%): C, 48.61; H, 2.91; N, 10.80. found (%): C, 48.69; H, 2.89; N, 10.78.

**UV–Vis absorption titration**

2000 μL solutions of the blank buffer and Ru (II) complexes sample (8 μM) were placed in the reference and sample cuvettes (1.0 cm path length), respectively, and then the first spectrum was recorded in the range of 200–600 nm. During the titration, we added an equal amount of DNA buffer to each cuvette to eliminate the absorbance of the DNA itself, and mixed the solution by inverting it repeatedly. Before recording the absorption spectrum, complex-DNA solutions were incubated for 5 min. We repeated the titration processes until there was no change in the spectrum of at least 4 titrations, demonstrating that binding saturation had been reached. At the end of each titration, Ru (II) complexes concentration change due to dilution is negligible.

**Cell Culture**

The Human glioblastoma cell line U87 MG cells were purchased from the Cell Bank of the Chinese Academy of Sciences (Shanghai, China). The cells were incubated in 25 mL cell culture flask with high glucose DMEM with 10% FBS and 1% penicillin-streptomycin solution. Cells were cultured in an incubator at 37 °C under a humidified atmosphere containing 5% carbon dioxide.

**Cytotoxicity Assay**

In vitro cytotoxicity of Ru1, Ru2, Ru3, Ru4 and DDP were measured by the CCK-8 assay. U87 MG cells were seeded into 96-well plates at a density of $10^4$ cells and 100 μL of DMEM in each well. After incubation for 24 h, tumor cells were treated by different concentration of Ru1, Ru2, Ru3, Ru4 and DDP for 24 h. 100 μL of DMEM (without FBS) containing 10% CCK-8 was added into each well. After 2 h of culture, the cytotoxicity was determined by the CCK-8 assay.

**Cellular Apoptosis**

U87 MG cells were seeded into 6-well plates at a density of $5\times10^5$ cells and 1 mL of DMEM in each well. After 24 h for incubation, tumor cells were treated by different concentration of Ru1 and DDP for 24 h. The old DMEM was transferred to a 15mL centrifuge tube. The cells were washed with PBS and digested with Trypsin Solution without EDTA. After digestion, the cells were transferred into the previous 15mL centrifuge tube for centrifugation at 2000 r/min for 5 min. After centrifugation, the supernatant was discarded. The cells were washed by PBS twice (centrifuged at 2000rpm for 5 min) and the cells were collected. 500 μL Binding Buffer was added to suspend the cells. Subsequently, 5 μL Annexin V-FITC and 5 μL PI were added and mixed at room temperature and out of light for 15 minutes. Flow cytometry was performed within 1 h.

**Live & Dead Viability Assay**

U87 MG cells were seeded at a density of $1\times10^5$ cells/well in 6-well plates overnight. The cells were administered with Ru1, PBS and DDP for 24 h. Next, the cells were stained with AM/PI solution (2 μL AM ,8 μL PI, 10 mL PBS) for 30 min and imaged by a fluorescent inverted microscope (AM Ex = 495 nm, Em = 520 nm; PI Ex = 530 nm, Em = 620 nm).

**Cell Cycle Analysis**

U87 MG cells were seeded at a density of $1\times10^5$ cells/well in 6-well plates and left to adhere overnight. The cells were treated with PBS, DDP and Ru1 for 24 h, after which cells were trypsinized, washed, and fixed with 70% alcohol at -4°C for 12 h. Next, the fixed cells were stained with PI/RNase A staining solution (50μL RNase A 450μL PI) for 45 min at 37°C in the dark. Flow cytometry was performed within 1 h.

**In Vivo Safety Evaluation of DDP and Ru1**

To investigate the in vivo toxicity of DDP and Ru1, mice were euthanized and the blood from each group was collected after treatment on day 10 for blood routine test and biochemistry tests. Meanwhile, the heart, liver, spleen, lung and kidney from each group were removed and stained by H&E for histological analysis.

**In Vivo Anti-Tumor Study**

To establish the tumor subcutaneous model, U87 MG cells ($5\times10^6$) were subcutaneously injected in the right back of male nude mice (20-22 g). When the volume of these tumors reached approximately 150mm$^3$, mice were randomly divided into three groups (4 in each) and respectively received the intravenous injection of DDP and Ru1 with a dosage of 5 mg /kg or PBS. The diameter of tumors was measured with a vernier caliper every 2 days along with therapy administration. The volumes of tumors were calculated via the formula: tumor volume = (length) × (width)$^2$/2. Mice body weight were measured every 2 days after treatment. All mice were sacrificed on day 10 and the final tumor weight was monitored directly. The tumors and major organs (heart, liver, spleen, lung and kidney) were excised and stored in 4 % paraformaldehyde for histological examination: hematoxylin and eosin (H&E) staining and TUNEL staining.

**Histopathological Examination**

Tumors and organs were embedded in paraffin and tissue sections of each group were stained with hematoxylin-eosin. The sections of H&E staining were observed by the optical microscope.

**Immunofluorescence Histochemical Analysis**

Tumors and major organs (heart, liver, spleen, lung and kidney) were fixed with 4.0% paraformaldehyde, embedded in paraffin, sectioned and stained with H&E. TUNEL staining was used to detect apoptotic cells according to a previously reported method.

**Statistical Analysis**

Analysis of variance (ANOVA) was performed for all data analysis and values were presented as means ± standard

deviation. Differences were considered statistically significant at $P < 0.05$ (*) $P < 0.01$ (**) and $P < 0.001$ (***). All the data was analyzed by SPSS 21.0.

## Conclusions

In Summary, we have successfully synthesized four new Ru (II) complexes, $[Ru(phen)_2podppz]^{2+}$, $Ru(bpy)_2podppz]^{2+}$, $[Ru(phen)_2ppip]^{2+}$, $[Ru(bpy)_2ppip]^{2+}$. They were characterized by ESI-MS, $^1H$ NMR, $^1H$-$^1H$ COSY NMR and elemental analysis. Firstly, the anti-tumor experiments in vitro and vivo confirmed that Ru1 exhibited excellent antitumor efficacy on GBM. Furthermore, we confirmed the strongest binding ability and the anti-tumor mechanism of Ru1 via DNA binding experiments and cell cycle experiments. Moreover, the study in vivo safety and biocompatibility of Ru1 was investigated and the results demonstrated that Ru1 could avoid any detectable side-effects compared with cisplatin. The results indicate that Ru1 is a very promising drug candidate and provide a new idea for the follow-up treatment of GBM.

## Conflicts of interest

There are no conflicts to declare.

## Acknowledgements

This work was supported by the National Nature Science Foundation of China (21671150, 81860547, 21877084, 81573008), Joint projects of Health and Family Planning Committee of Pudong New Area (PW2017D-10), the Fundamental Research Funds for the Central Universities (kx0150720173382), Science and Technology Commission of Shanghai Municipality Fund (16DZ1930509), Science and Technology Commission of Shanghai Municipality Fund (No. 16DZ1930509), and Shanghai Pudong New Area Science and Technology Development Fund, Innovation Fund (PKJ2017-Y18).

## Notes and references

1 Q. T. Ostrom, H. Gittleman, J. Xu, C. Kromer, Y. Wolinsky, C. Kruchko and J. S. Barnholtz-Sloan, *Neuro-Oncol.*, 2016, **18,** v1-v75.
2 A. Omuro, K. Beal, K. McNeill, R. J. Young, A. Thomas, X. Lin, R. Terziev, T. J. Kaley, L. M. DeAngelis, M. Daras, I. T. Gavrilovic, I. Mellinghoff, E. L. Diamond, A. McKeown, M. Manne, A. Caterfino, K. Patel, L. Bavisotto, G. Gorman, M. Lamson, P. Gutin, V. Tabar, D. Chakravarty, T. A. Chan, C. W. Brennan, E. Garrett-Mayer, R. A. Karmali and E. Pentsova, *J. Clin. Oncol.*, 2018, **36**, 1702-1709.
3 R. Stupp, M. Brada, M. J. van den Bent, J. C. Tonn, G. Pentheroudakis and E. G. W. Grp, *Ann. Oncol.*, 2014, **25**, 93-101.
4 B. Rosenberg, L. Vancamp, J. E. Trosko and V. H. Mansour, *Nature*, 1969, **222**, 385-386.
5 S. A. Funt and J. E. Rosenberg, *Nat. Rev. Clin. Oncol.*, 2017, **14**, 221-234.
6 A.M. Florea and D. Busselberg, *Cancers*, 2011, **3**, 1351-1371.
7 Y. R. Zheng, K. Suntharalingam, T. C. Johnstone, H. Yoo, W. Lin, J. G. Brooks and S. J. Lippard, *J. Am. Chem. Soc.*, 2014, **136**, 8790-8798.
8 K. Suntharalingam, Y. Song and S. J. Lippard, *Chem. Commun.*, 2014, **50**, 2465-2468.
9 D. Yue, S. Xu, Q. Wang, X. Li, Y. Shen, H. Zhao, C. Chen, W. Mao, W. Liu, J. Liu, L. Zhang, H. Ma, Q. Li, Y. Yang, Y. Liu, H. Chen and C. Wang, *Lancet. Respir. Med.*, 2018, **6**, 863-873.
10 L. Duan, A. Fischer, Y. Xu and L. Sun, *J. Am. Chem. Soc.*, 2009, **131**, 10397-10399.
11 M. R. Gill and J. A. Thomas, *Chem. Soc. Rev.*, 2012, **41**, 3179-3192.
12 S. Antony, J. B. Aitken, S. Vogt, B. Lai, T. Brown, L. Spiccia and H. H. Harris, *J. Biol. Inorg. Chem.*, 2013, **18**, 845-853.
13 A. Notaro and G. Gasser, *Chem. Soc. Rev.*, 2017, **46**, 7317-7337.
14 N. Muhammad and Z. Guo, *Curr. Opin. Chem. Biol.*, 2014, **19**, 144-153.
15 S. M. Meier-Menches, C. Gerner, W. Berger, C. G. Hartinger and B. K. Keppler, *Chem. Soc. Rev.*, 2018, **47**, 909-928.
16 J. Shen, H.C. Kim, J. Wolfram, C. Mu, W. Zhang, H. Liu, Y. Xie, J. Mai, H. Zhang, Z. Li, M. Guevara, Z.W. Mao and H. Shen, *Nano. Lett.*, 2017, **17**, 2913-2920.
17 W. Sun, S. Li, B. Häupler, J. Liu, S. Jin, W. Steffen, U. S. Schubert, H.J. Butt, X.J. Liang and S. Wu, *Adv. Mater.*, 2017, **29**, 1603702.
18 J.H. Liang, Y. Zheng, X.W. Wu, C.P. Tan, L.N. Ji and Z.W. Mao, *Adv. Sci.*, 2019, **7**, 1901992-1902005.
19 X. Meng, M. L. Leyva, M. Jenny, I. Gross, S. Benosman, B. Fricker, S. Harlepp, P. Hebraud, A. Boos, P. Wlosik, P. Bischoff, C. Sirlin, M. Pfeffer, J. P. Loeffler and C. Gaiddon, *Cancer. Res.*, 2009, **69**, 5458-5466.
20 J. Q. Wang, P. Y. Zhang, L. N. Ji and H. Chao, *J. Inorg. Biochem.*, 2015, **146**, 89-96.
21 M. Wumaier, J. J. Shi, T. M. Yao, X. C. Hu, R. R. Gao and S. Shi, *J. Inorg. Biochem.*, 2019, **196**, 110681-110691.
22 M. R. Gill and J. A. Thomas, *Chem. Soc. Rev.*, 2012, **41**, 3179-3192.
23 W.L. Wang, Z. Guo, Y. Lu, X. C. Shen, T. Chen, R. T. Huang, B. Zhou, C. Wen, H. Liang and B.P. Jiang, *ACS. Appl. Mater. Inter.*, 2019, **11**, 17294-17305.
24 H. Huang, P. Zhang, B. Yu, Y. Chen, J. Wang, L. Ji and H. Chao, *J. Med. Chem.*, 2014, **57**, 8971-8983.
25 F. E. Poynton, S. A. Bright, S. Blasco, D. C. Williams, J. M. Kelly and T. Gunnlaugsson, *Chem. Soc. Rev.*, 2017, **46**, 7706-7756.
26 L. Tan, J. Shen, J. Liu, L. Zeng, L. Jin and C. Weng, *Dalton. Trans.*, 2012, **41**, 4575-4587.
27 J. L. Yao, X. Gao, W. L. Sun, X. Z. Fan, S. Shi and T. M. Yao, *Inorg. Chem.*, 2012, **51**, 12591-12593.
28 D. C. Kennedy, C. S. McKay, L. l. Tay, Y. Rouleau and J. P. Pezacki, *Chem. Commun.*, 2011, **47**, 3156-3158.
29 N. Ranjan, G. Fulcrand, A. King, J. Brown, X. Jiang, F. Leng and D. P. Arya, *Medchemcomm*, 2014, **5**, 816-825.
30 S. Zhang, Q. Wu, H. Zhang, Q. Wang, X. Wang, W. Mei, X. Wu and W. Zheng, *J. Inorg. Biochem.*, 2017, **176**, 113-122.
31 Z.P. Zeng, Q. Wu, F. Y. Sun, K.D. Zheng and W. J. Mei, *Inorg. Chem.*, 2016, **55**, 5710-5718.
32 B. P. Sullivan, D. J. Salmon, T. J. Meyer, *Inorg. Chem.*, 1978, **17**, 3334-3341.
33 C. Hiort, P. Lincoln and B. Nordén, *J. Am. Chem. Soc.*, 1993, **115**, 3448-3454.
34 X. W. Liu, J. Li, H. Li, K.C. Zheng, H. Chao, L. N. Ji, *J. Inorg. Biochem.*, 2005, **99**, 2372-2380.
35 J. Z. Wu, B. H. Ye, L. Wang, L. N. Ji, J. Y. Zhou, R. H. Li and Z. Y. Zhou, *J. Chem. Soc., Dalton Trans.*, 1997, **8**, 1395-1401.
36 X. W. Liu, J. Li, H. Li, K. C. Zheng, H. Chao and L. N. Ji, *J. Inorg. Biochem.*, 2005, **99**, 2372-2380.

View Article Online
DOI: 10.1039/D0DT01877E

37 R. K. Dubey, M. Niemi, K. Kaunisto, K. Stranius, A. Efimov, N. V. Tkachenko and H. Lemmetyinen, *Inorg. Chem*., 2013, **52**, 9761-9773.
38 J. Q. Cao, Q. Wu, W. J. Zheng, L. Li and W. J. Mei, *RSC Adv.*, 2017, **7**, 26625-26632.
39 L. N. Ji, X. H. Zou and J. G. Liu, *Coordin. Chem. Rev.*, 2001, **216**, 513-536.
40 S. Shi, X. Gao, H. Huang, J. Zhao and T. Yao, *Chem-Eur. J.*, 2015, **21**, 13390-13400
41 S. Shi, T. Xie, T. M. Yao, C. R. Wang, X. T. Geng, D. J. Yang, L. J. Han, L. N. Ji, *Polyhedron*, 2009, **28**, 1355-1361.
42 A. W. Scott, B. M. Tyler, B. C. Masi, U. M. Upadhyay, Y. R. Patta, R. Grossman, L. Basaldella, R. S. Langer, H. Brem and M. J. Cima, *Biomaterials*, 2011, **32**, 2532-2539

View Article Online
DOI: 10.1039/D0DT01877E

Ru1 could most effectively inhibit tumor growth and avoid any detectable side-effects compared with other ruthenium (II) complexes and cisplatin, demonstrating its potential to be an exciting new drug candidate for glioblastoma treatment.